10-23-2020

# An Update of Seismic Monitoring and Research in the Vicinity of the Paducah Gaseous Diffusion Plant: January 2018–December 2019

Zhenming Wang
*University of Kentucky*, zhenming.wang@uky.edu

N. Seth Carpenter
*University of Kentucky*, seth.carpenter@uky.edu

Edward W. Woolery
*University of Kentucky*, ewoolery@uky.edu

**Kentucky Geological Survey**
William C. Haneberg, State Geologist and Director
University of Kentucky, Lexington

# An Update of Seismic Monitoring and Research in the Vicinity of the Paducah Gaseous Diffusion Plant: January 2018–December 2019

**Zhenming Wang, N. Seth Carpenter, and Edward W. Woolery**

Report of Investigations 12 doi.org/10.13023/kgs.ri12.13 Series XIII, 2020

## Our Mission

The Kentucky Geological Survey is a state-supported research center and public resource within the University of Kentucky. Our mission is to support sustainable prosperity of the commonwealth, the vitality of its flagship university, and the welfare of its people. We do this by conducting research and providing unbiased information about geologic resources, environmental issues, and natural hazards affecting Kentucky.

## Earth Resources—Our Common Wealth

**www.uky.edu/kgs**



## Technical Level

General Intermediate Technical

## Statement of Benefit to Kentucky

Continuing efforts to monitor earthquakes and conduct research have enhanced our understanding of seismic hazards in western Kentucky, which in turn has contributed to a sound scientific basis for developing design ground motions for buildings and facilities at the Paducah Gaseous Diffusion Plant and for western Kentucky, in general.

**ISSN 0075-5591**

# Contents



# Figures

# Tables

# An Update of Seismic Monitoring and Research in the Vicinity of the Paducah Gaseous Diffusion Plant: January 2018–December 2019

Zhenming Wang, N. Seth Carpenter, and Edward W. Woolery

## Abstract

From January 2018 to December 2019, the Kentucky Geological Survey monitored earthquakes and conducted research on seismic hazards in the vicinity of the Paducah Gaseous Diffusion Plant, a former uranium enrichment facility, in McCracken County, western Kentucky. Six hundred forty-four earthquakes with magnitude between 0.5 and 3.7 were recorded in the area during this period. Research focused on the influence of the thick sediments on earthquake ground motion, the so-called site response, through theoretical and data analysis of borehole seismic records. Our research has shown that the National Earthquake Hazards Reduction Program site classification, which is based on $V_s30$, and correction factors currently being used in earthquake engineering design and other safety evaluations are not appropriate to account for site response in the area.

## Introduction

As part of a Phase III project supported by the U.S. Department of Energy under award number DE-EM0004146 through the Kentucky Research Consortium for Energy and Environment, the Kentucky Geological Survey is monitoring the seismicity and conducting research on seismic hazards in the area surrounding the plant. Phase I of the project was from 2003–2007 and Phase II from 2009–2012. Phase I results are presented in Wang (2003, 2005, 2006, 2007, 2008), Wang and others (2003), Wang and Ormsbee (2005), Wang and Woolery (2006, 2008), and Woolery and others (2008). Phase II results are in Wang (2010, 2011), Wang and Lu (2011), Wang and Cobb (2012), Wang and others (2012), and Wang and Woolery (2013). The most significant outcomes from the first two phases are summarized in Wang and others (2019).

This report summarizes the efforts from January 2018–December 2019.

## Seismic and Strong-Motion Network Operation and Data

The Kentucky Geological Survey operates the Kentucky Seismic and Strong-Motion Network in the vicinity of the Paducah Gaseous Diffusion Plant. Figure 1 shows the current station and instrumentation configuration, which focuses on monitoring the New Madrid Seismic Zone. Seven of the stations operate seismometers for detecting weak seismic events, and 10 stations operate at least one strong-motion accelerometer to record on-scale strong ground motions in the event of a nearby large earthquake. Recordings from five of the stations are telemetered to KGS over the inter-

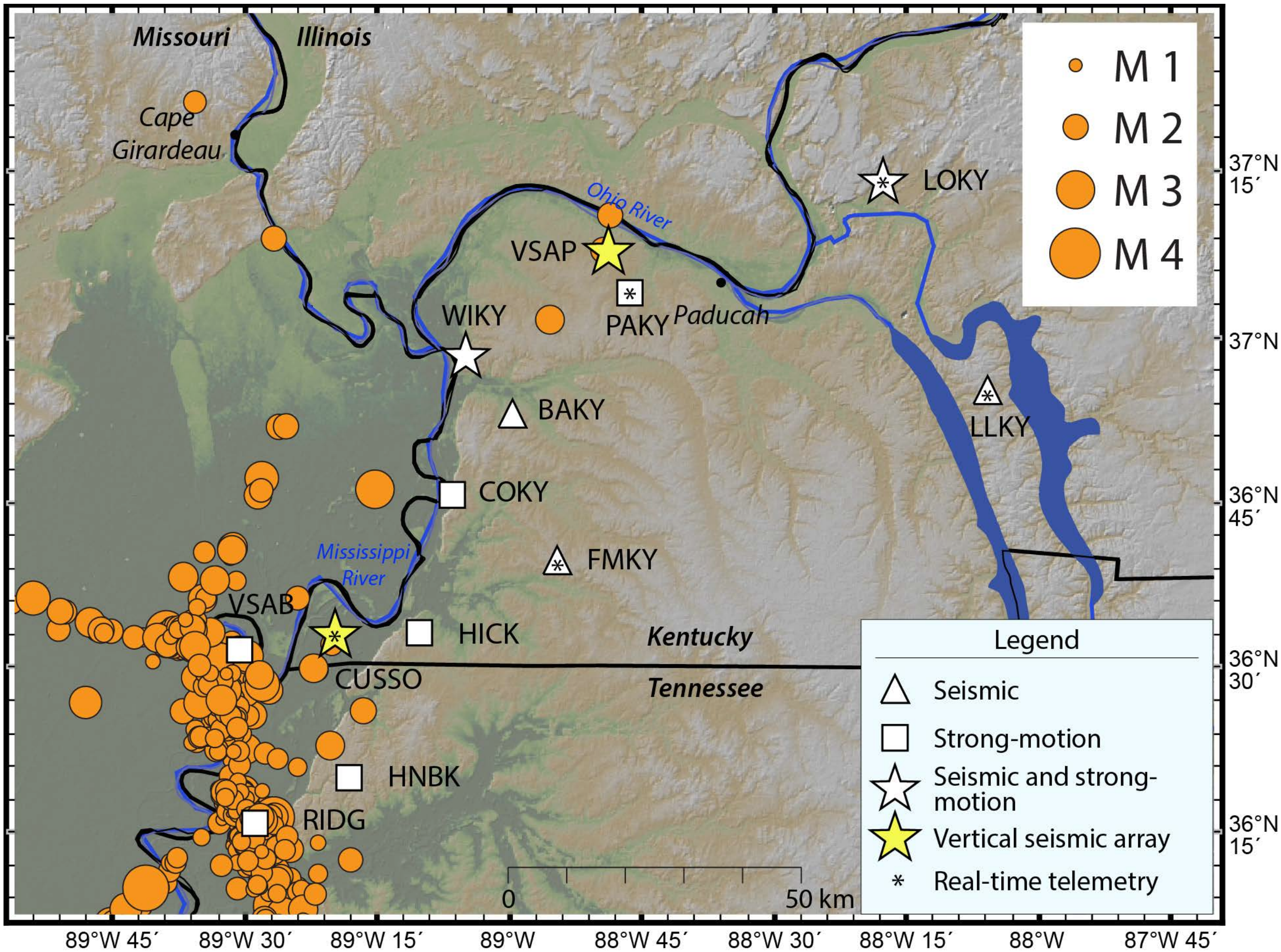


Figure 1. Seismic and strong-motion stations operated in the vicinity of the Paducah Gaseous Diffusion Plant, the location of which coincides with station VSAP. Also shown is seismicity that occurred from January 2018 through December 2019.

net; the remaining stations are stand-alone, and are visited approximately every other month to download recordings. The network stations, particularly the weak-motion ones, record earthquakes on local and global scales. The real-time recordings are shared with the neighboring seismic monitoring network operated by the University of Memphis. Figure 1 also shows the locations and magnitudes of earthquakes that occurred in the area between January 2018 and December 2019.

## Ground-Motion Site Response

Ground motion can be significantly modified by near-surface, low-velocity materials in terms of spectral content, amplitude, and duration: the so-called site response or site effect. Site response is a great concern in earthquake engineering. For example, the resonance of soft lake sediments caused significant damage to buildings of five to 16 stories in Mexico City during the 1985 Michoacán earthquake (M8.0) (Seed and others, 1988). Site response has also been observed worldwide during strong earthquakes, as in 1989 in Loma Prieta, California (M6.9) (Borcherdt and Glassmoyer, 1992), in 1994 in Northridge, California (M6.7) (Hartzell and others, 1996), in 2008 in Wenchuan, China (M8.0) (Lu and others, 2010), and in 2015 in Gorkha, Nepal (M7.8) (Asimaki and others, 2017). Site response is also a concern in Kentucky because many communities, such as Owensboro and Paducah, are underlain by soft sediments overlying hard bedrock. As shown by Woolery and others (2008), site response caused by soft sediments over hard bedrock resulted in significant damage in Maysville, Kentucky, during the 1980 Sharpsburg earthquake (M 5.3).

Figure 2 shows the depth to bedrock in the New Madrid Seismic Zone, Upper Mississippi Embayment, and Jackson Purchase Region of western Kentucky. The Jackson Purchase Region is underlain by thick unlithified sediments, ranging from 0 m in the east and north to about 600 m to the southwest, over Paleozoic bedrock. Figure 3 illustrates the simplified 3-D stratigraphy of Cretaceous to Holocene sediments of the Jackson Purchase.

In the early 1990s, Harris (1992) and Harris and others (1994) studied site response in the Paducah area. They obtained shear-wave velocity profiles at many sites throughout the Upper Mississippi Embayment, including the Jackson Purchase Region, using seismic reflection/refraction methods (Street and others, 1997a, c, 2001). The first borehole strong-motion array, VSAP (Figs. 1, 4), was installed at the gaseous diffusion plant in early 1990 and obtained its first strong-motion recordings from the Feb. 5, 1994, earthquake (4.2 $m_{b,Lg}$) in southern Illinois (Street and others, 1997b) (Fig. 5). The second borehole array, the Central U.S. Seismic Observatory (Figs. 1, 4), was installed in 2009 in Sassafras Ridge, Fulton County, Kentucky (Woolery and others, 2016a, b). Figure 6 shows waveforms recorded on the full CUSSO array from the Feb. 28, 2011, M 4.7 Arkansas earthquake. Thus, a significant database has been accumulated and provides an opportunity for a systematic study of site response in the central United States, the Jackson Purchase Region in particular.

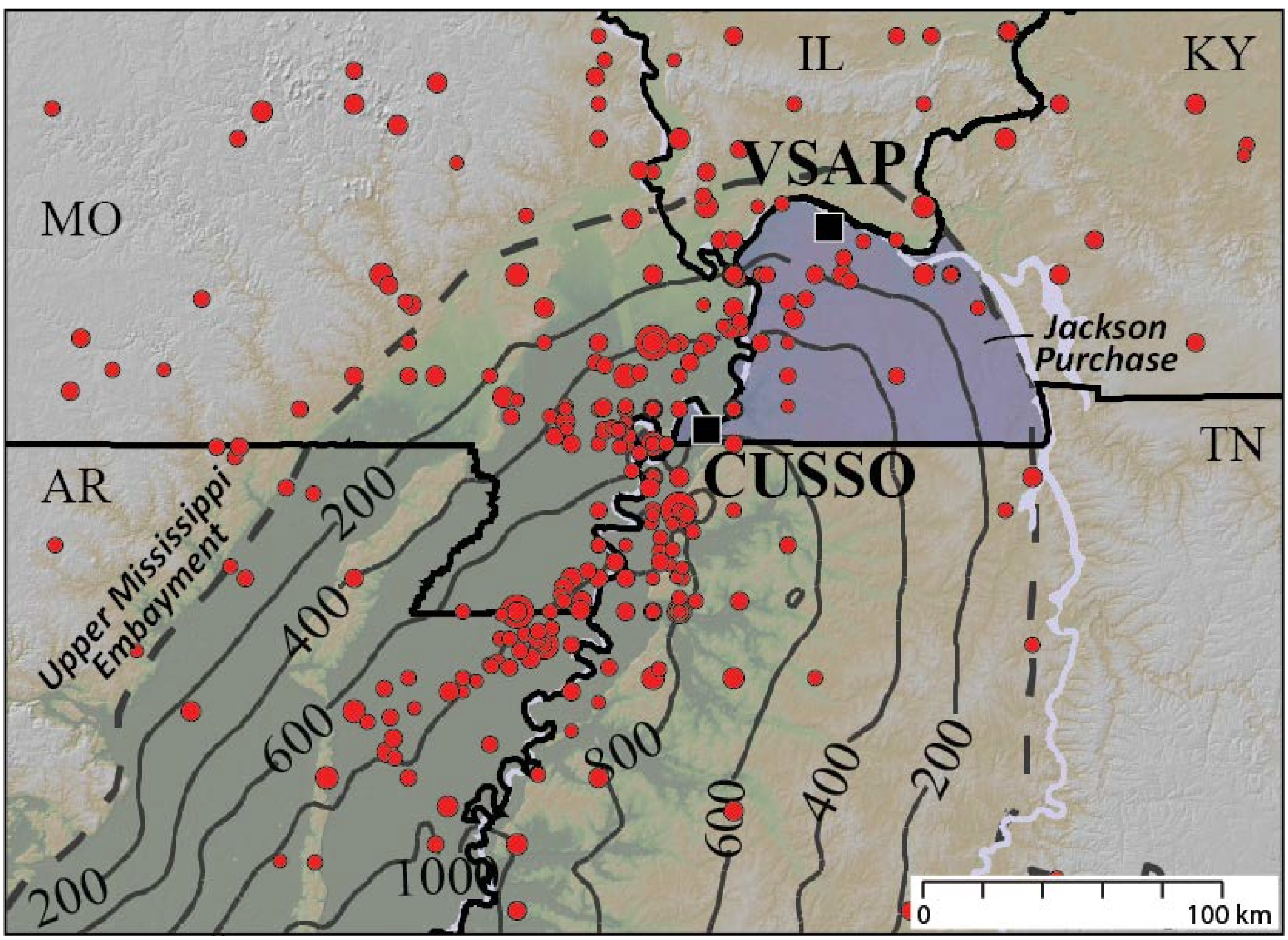


Figure 2. Locations of vertical seismic arrays CUSSO and VSAP in the Upper Mississippi Embayment, New Madrid Seismic Zone, and Jackson Purchase Region of western Kentucky (depth to bedrock contours in meters). Seismicity in red.

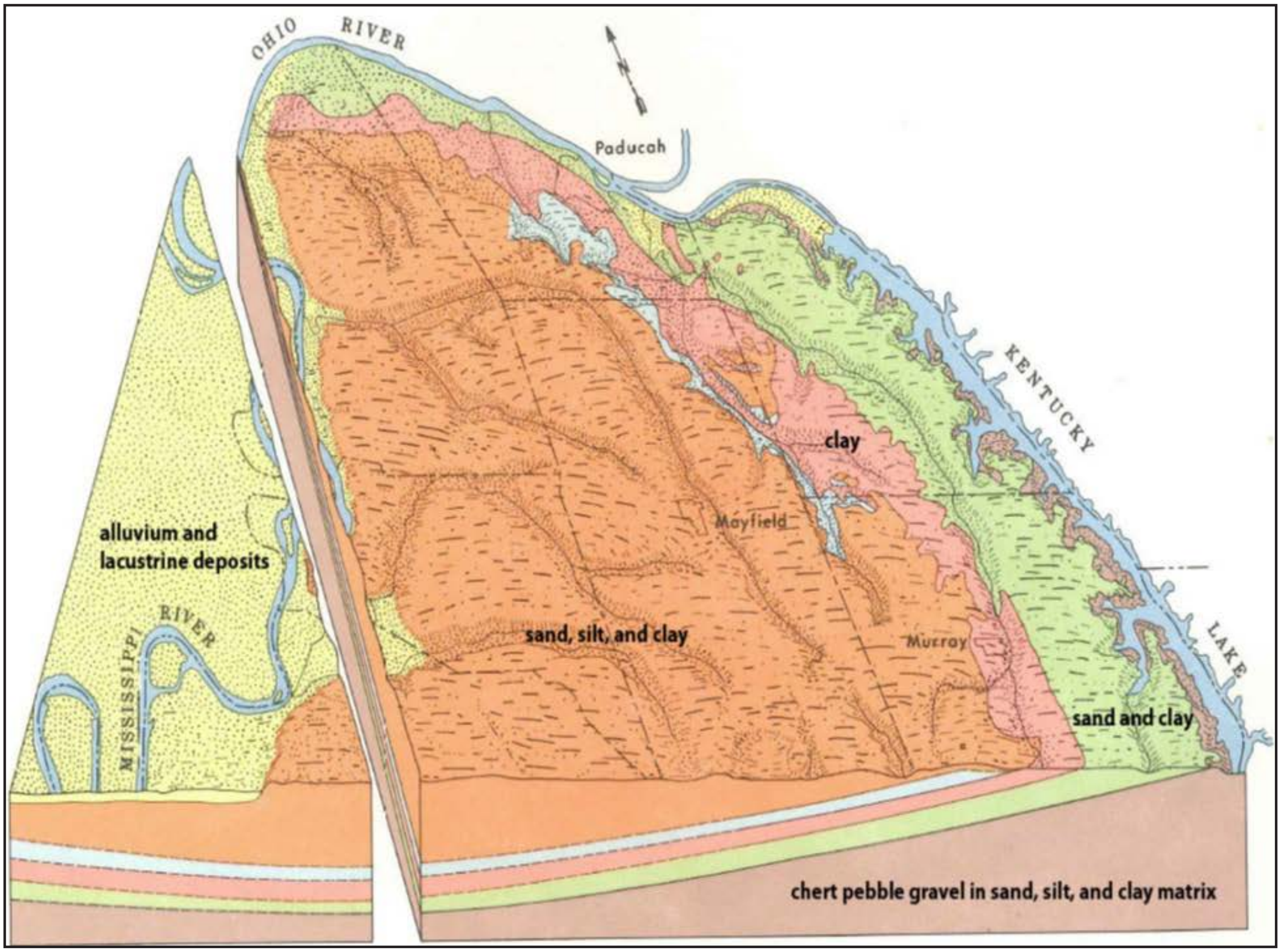


Figure 3. General stratigraphy of Cretaceous to Holocene consolidated and unconsolidated sediments in the northern part of the Mississippi Embayment. Modified from Olive (1972).

## Site-Response Assessments

Site response is a complex 3-D wave-propagation phenomenon (Fig. 7a). There are two broad categories of approaches for assessing site response: empirical and theoretical. The traditional empirical method is the soil-to-rock spectral ratio (Borcherdt, 1970):

$$SSR = \frac{A_S}{A_R} \quad (1)$$

where $A_S$ and $A_R$ are the Fourier spectral amplitudes of ground motion on soil and reference rock sites (Fig. 7b), respectively. This empirical method has been widely used in assessing site response. The main limitations of this approach are lack of observations and difficulty selecting the reference site.

As shown in Figure 7b, site response can also be empirically assessed by determining borehole ground motions as the ratio of the amplitude spectrum of the surface horizontal S-wave *($H_S$)* to that in the bedrock *($H_B$):*

$$TF_T = \frac{H_S}{H_B} \quad (2)$$

Equation 2 is the empirical SH-wave transfer function. Carpenter and others (2018) derived this function at VSAP and CUSSO from borehole data (Fig. 8).

Another empirical method for assessing site response is the horizontal-to-vertical spectral ratio of earthquake S-wave recordings at a single station (Carpenter and others, 2018, 2020). Lermo and Chávez-García (1993) were the first to dem-

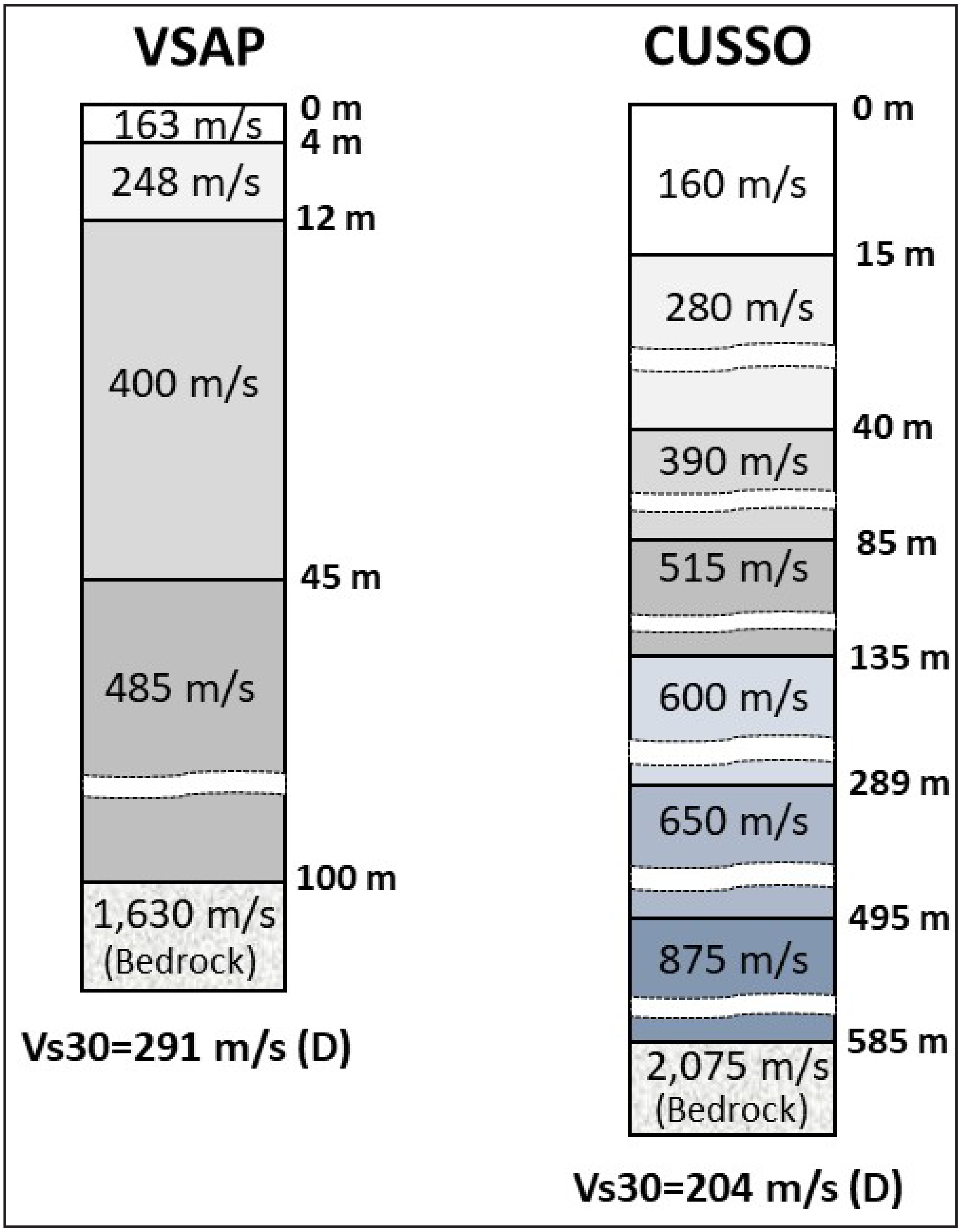


Figure 4. Shear-wave velocity structures at stations VSAP and CUSSO.

onstrate that single-station spectral ratios formed by the ratio of the horizontal-component S-wave spectrum to that of the vertical component could be used to estimate site response in the Mexico City area. Zhao and others (2006) used S-wave HVSR observations from Japan for site classifications and demonstrated that these spectral ratios revealed the fundamental frequencies at more than 600 K-net stations in Japan. Woolery and others (2008) and Zandieh and Pezeshk (2011) analyzed HVSRs of S-waves from small to moderate earthquakes in the central United States and found that the HVSR curves are comparable to site resonance curves. Carpenter and others (2018, 2020) further evaluated the S-wave HVSR and its potential application for site-response assessment and found that a correction factor of about 1.5 is needed in order to use the S-wave HVSR as an empirical transfer function at the fundamental site frequency. Figure 9 shows the corrected S-wave HVSR curves for stations VSAP and CUSSO.

As shown in Figure7a, 3-D ground-motion modeling is the best theoretical method for assessing site response (see, for example, Olsen, 2000). Some recent examples are discussed in Saikia and others (2006), Macpherson and others (2010), and Ramirez-Guzman and others (2015); they conducted 3-D ground-motion modeling to explore site responses in the New Madrid Seismic Zone.

As computational power has dramatically increased in recent decades, 3-D ground-motion modeling has also advanced greatly. Rodgers and others (2019) used the supercomputer at the Lawrence Berkeley National Laboratory to simulate ground motions with frequencies up to 5 Hz and sediment shear-wave velocities down to 500 m/s.

Although 3-D modeling is widespread, its application in site-response quantification for en-

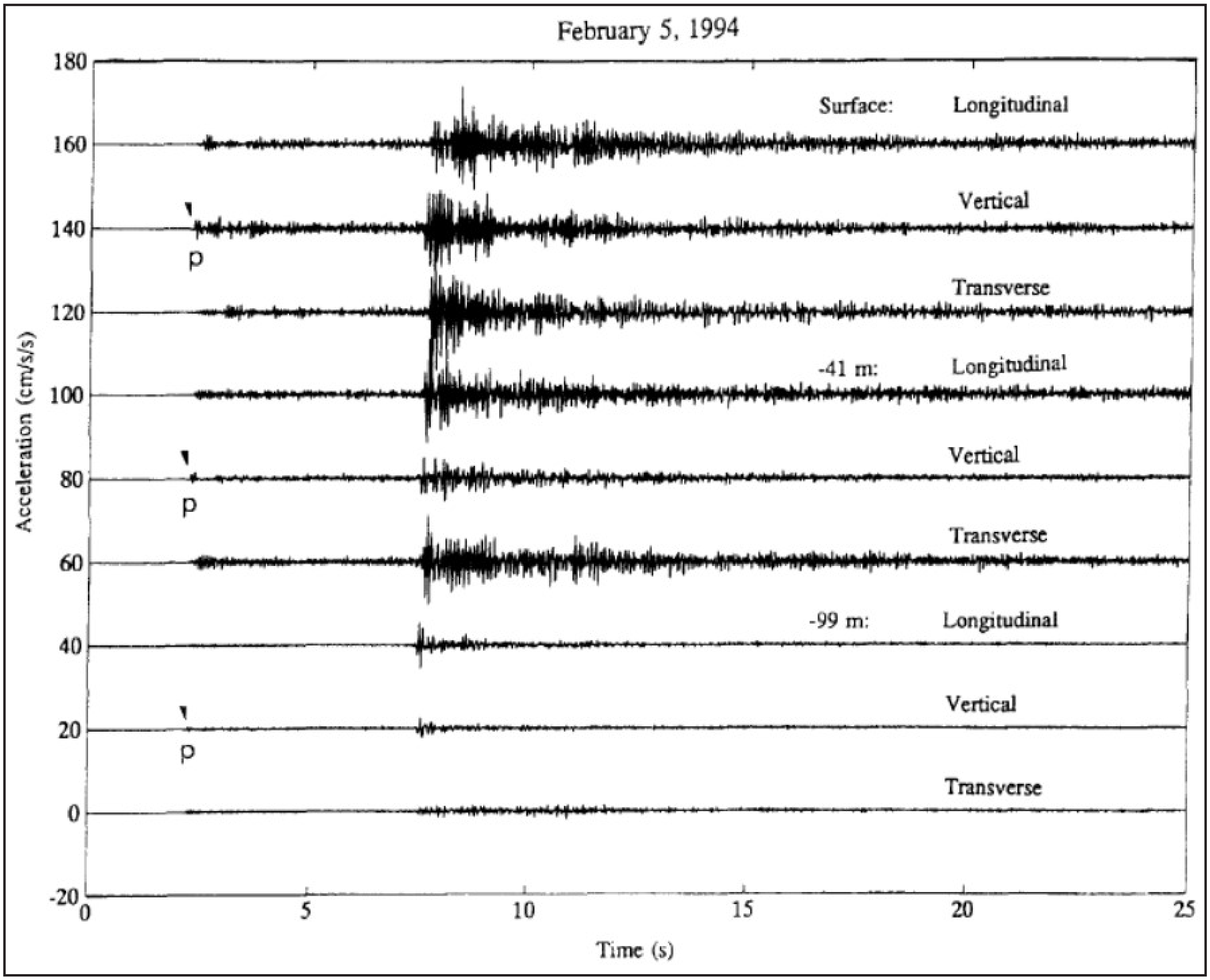


Figure 5. Accelerograms recorded at station VSAP for the southern Illinois earthquake of Feb. 5, 1994.

gineering purposes is still limited, particularly by inaccurate basin models, low earth-model resolution, low maximum frequencies that can be modeled, and an inability to properly account for the effects of soil nonlinearity. Therefore, 1-D modeling, using the equivalent linear approach—in particular, SHAKE91 by Idriss and Sun (1992)—is still predominantly used to estimate site response for engineering applications.

For a linear 1-D layered model (Fig. 7b), horizontally polarized S-wave (i.e., SH-mode) propagation can be quantified using Thomson-Haskell propagator matrices (Haskell, 1953, 1960). For a single sediment layer over bedrock, the fundamental site period $(T_f)$ or frequency $(f_0)$ can be calculated:

$$T_f = \frac{4H}{V_{SS}} \quad \text{or} \quad f_0 = \frac{V_{SS}}{4H} \tag{3}$$

where $V_{SS}$ and $H$ are shear-wave velocity and thickness of sediment, respectively. The peak amplification at $T_f$ can be calculated:

$$A_0 = \frac{1}{\dfrac{\rho_S V_{SS}}{\rho_R V_{SR}} + \dfrac{\pi \xi_S}{2}} \tag{4}$$

where $\rho_S$ and $\xi_S$ are the density and damping ratio of sediment, respectively, and $V_{SR}$ and $\rho_R$ are shear-wave velocity and density of bedrock, respectively.

Schnabel and others (1972) developed a computer program, SHAKE, to perform 1-D linear site-response analysis using Thomson-Haskell propa-

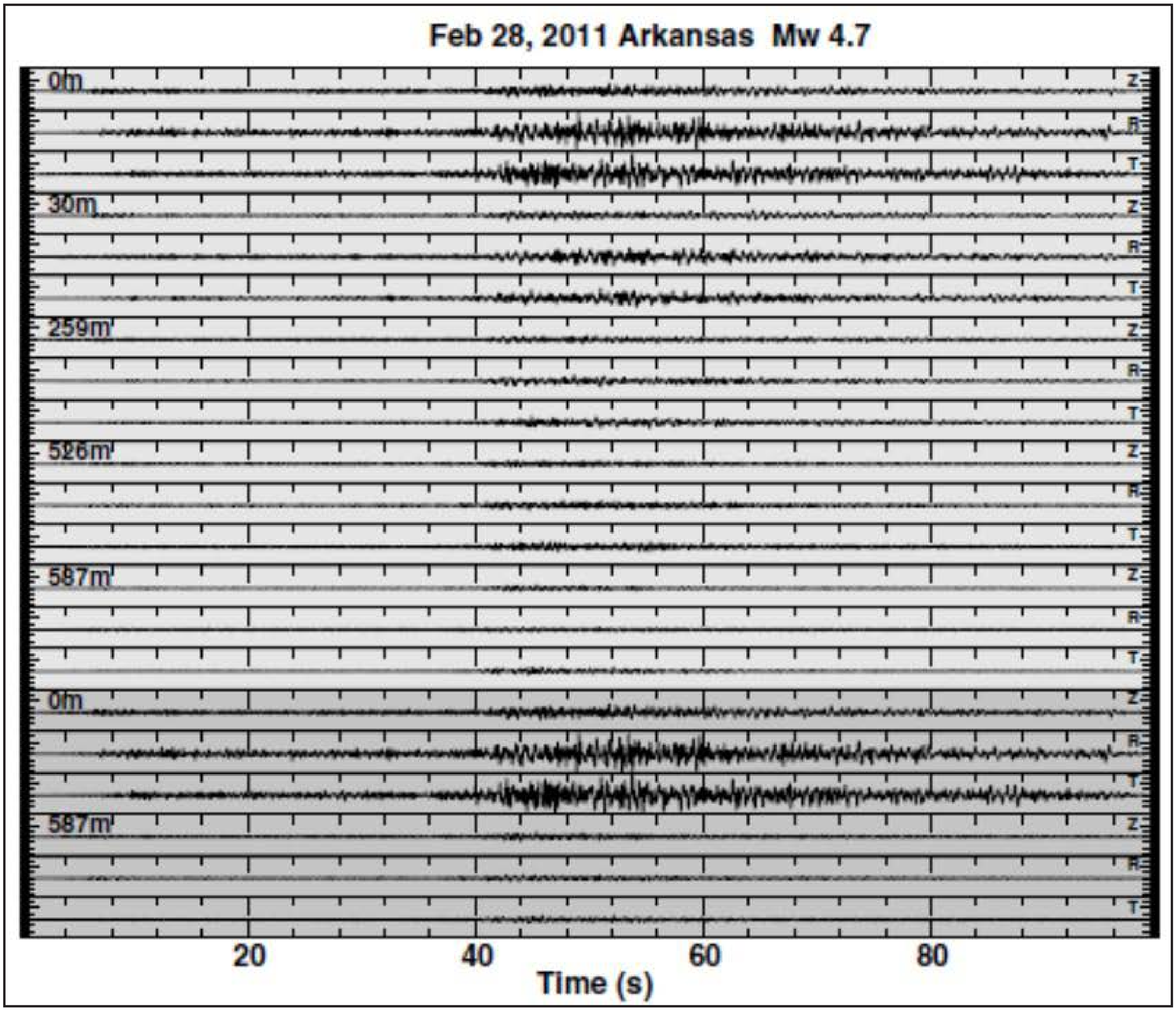


Figure 6. Waveforms recorded on the full CUSSO array from the Feb. 28, 2011, M4.7 Arkansas earthquake.

gator matrices. As shown by Hardin and Drnevich (1972), soils are nonlinear materials; consequently, Idriss and Sun (1992) modified SHAKE to create SHAKE91 and used it to account for the nonlinear behavior of soils, using an equivalent linear iterative procedure. Figure 10 shows the spectral amplifications of linear and equivalent linear site-response analyses for the shear-wave velocity structures at stations VSAP and CUSSO (Fig. 4). The equivalent linear analyses were performed for the input motions scaled to 0.20 g and 0.40 g PGA, respectively, using STRATA (Kottke and Rathje, 2009). As shown in Figure 10, soil nonlinearity significantly affects site response: It lowers the resonance frequencies and dampens the higher-mode amplitudes with increasing input PGA.

Figure 11 compares the site response from 1-D linear analysis with the empirical transfer functions and corrected HVSR curves for stations VSAP and CUSSO. The figure shows that the base-mode frequencies (i.e., the fundamental site frequencies) are similar to the empirical transfer functions, and the associated peak amplifications are slightly different from the empirical transfer functions. In other words, site response can be assessed by empirical and 1-D theoretical methods. Also, soil nonlinearity significantly damped higher-mode amplitudes (Fig. 10). Thus, for engineering applications (i.e.,

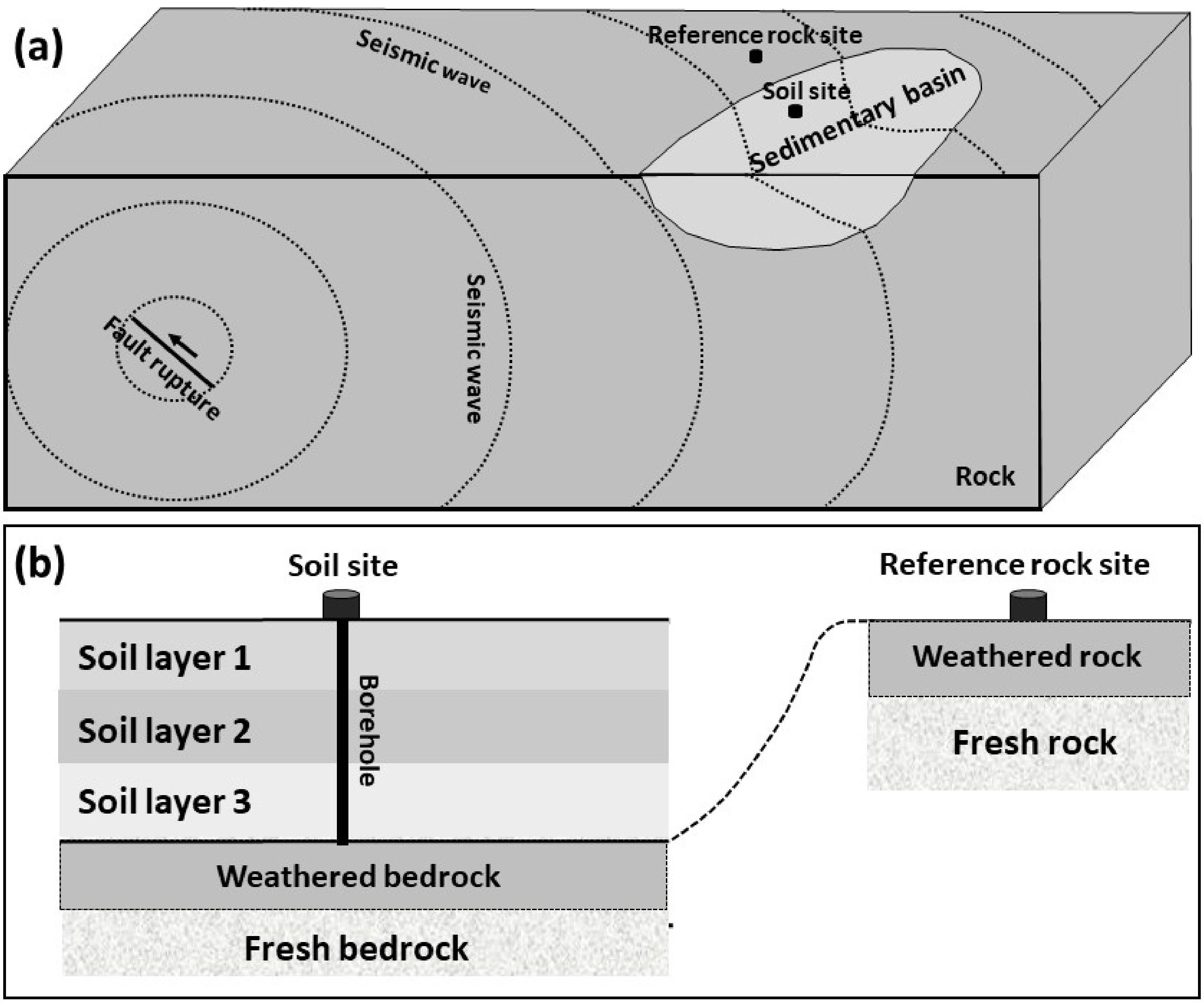


Figure 7. Schematic seismic-wave propagation in 3-D earth (a) and a simplified 1-D model for soil and reference rock sites (b).

the strong ground motions with PGA greater than 0.05 g), site response can be quantified by two parameters: the fundamental site frequency ($f_0$) or period ($T_f$) and its peak amplification ($A_0$).

## National Earthquake Hazards Reduction Program Site Classification and Correction Factors

The time-averaged shear-wave velocity for the top 30 m of soils and rocks, $V_s30$, has been used as the primary parameter to account for site response in engineering seismic design in the United States (Table 1) (Building Seismic Safety Council, 1995, 2015). The time-averaged shear-wave velocity is defined as:

$$V_S30 = \frac{\sum_{i=1}^{n} d_i}{\sum_{i=1}^{n} \frac{d_i}{v_{si}}} \quad (5)$$

where $d_i$ is the thickness of any layer between 0 and 30 m and $v_{si}$ is the shear-wave velocity in m/s. The site correction factors (Tables 2–3), based on $V_s30$ and input ground-motion level, have been developed and used for engineering design, such as those by the American Society of Civil Engineers (2010) and the International Code Council (2011).

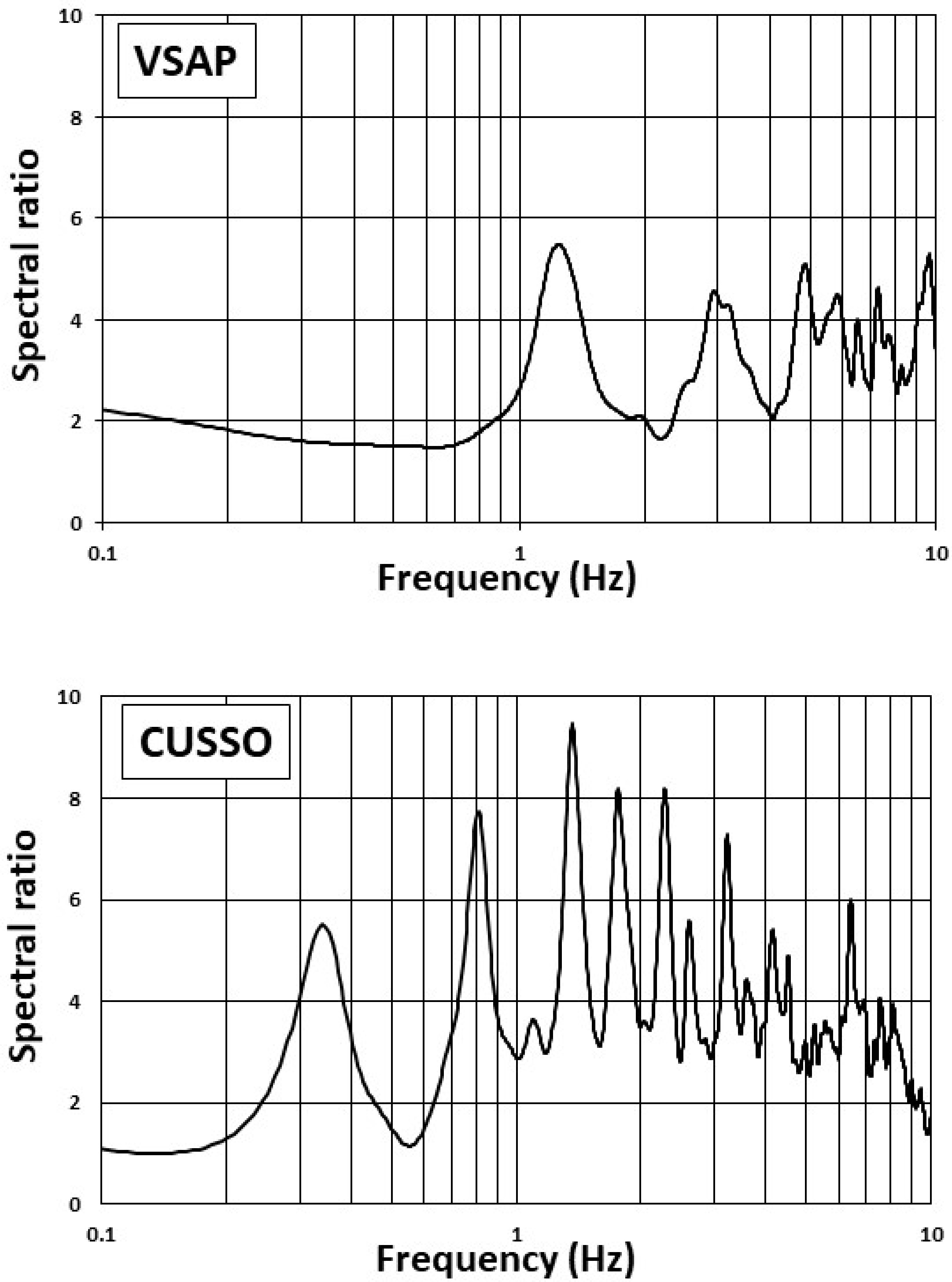


Figure 8. Mean spectral ratios from recordings (empirical SH-wave transfer function) at stations VSAP and CUSSO.

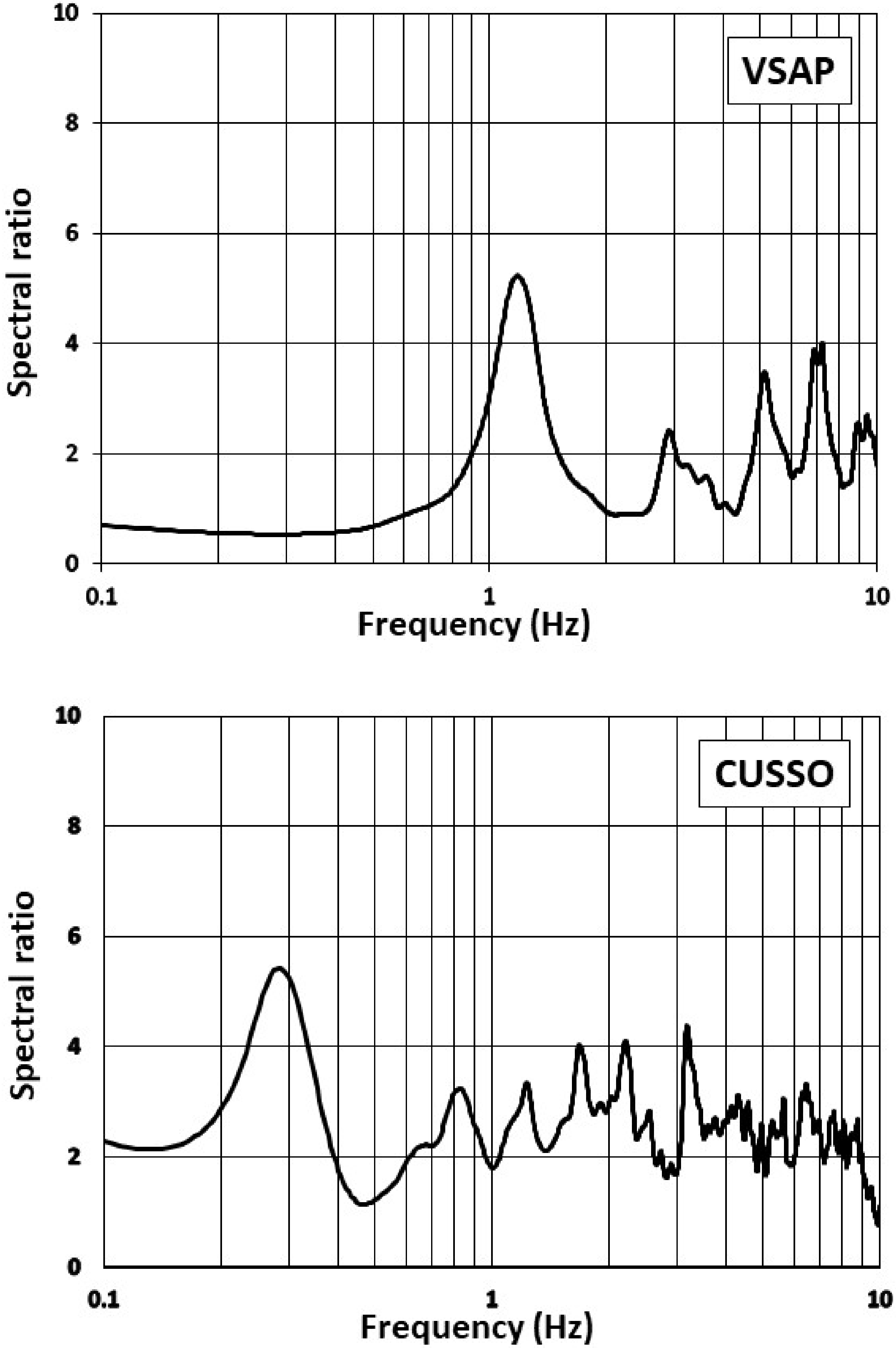


Figure 9. Corrected S-wave HVSR curves for stations VSAP and CUSSO.

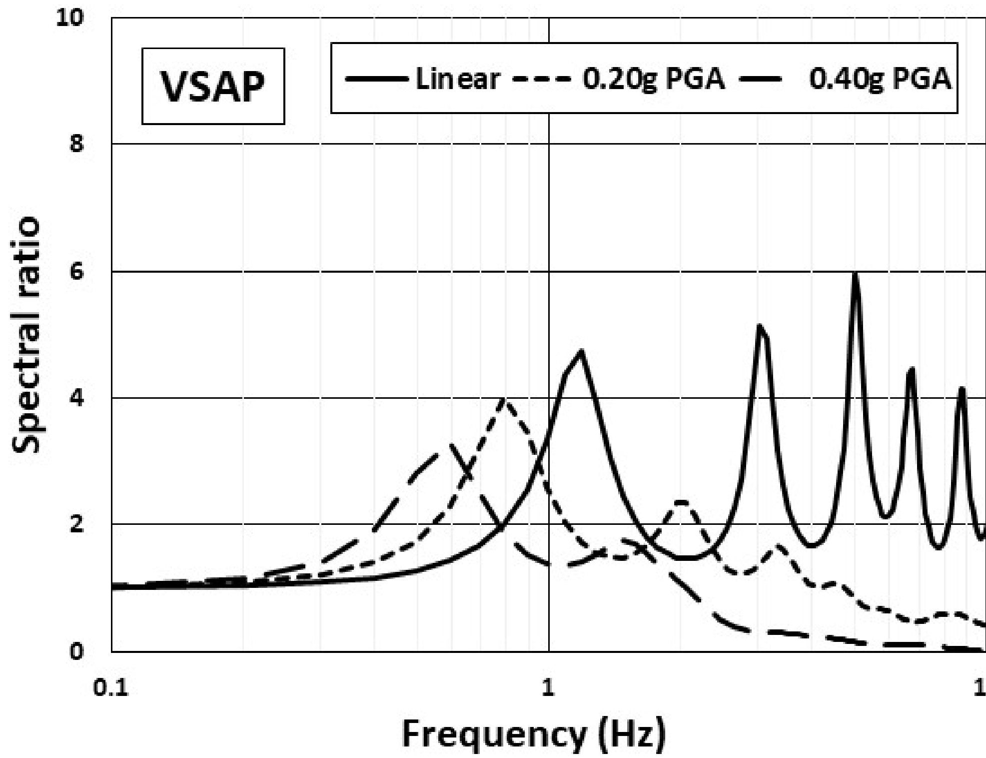


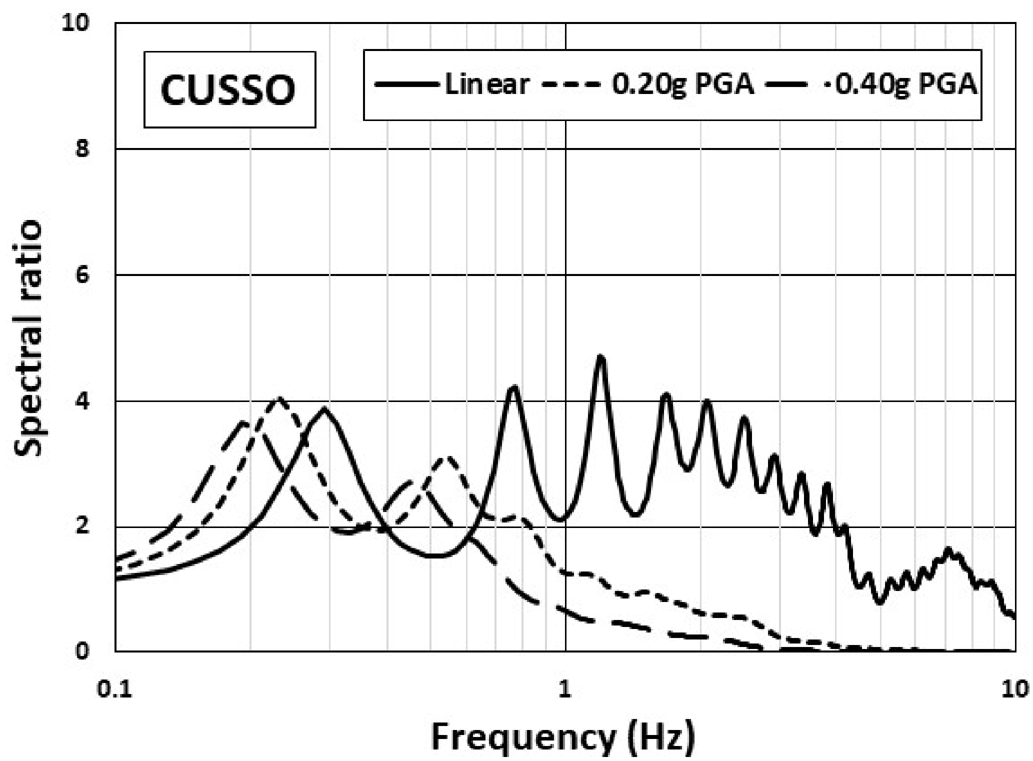


Figure 10. Linear and equivalent-linear site-response spectral curves for stations VSAP and CUSSO.

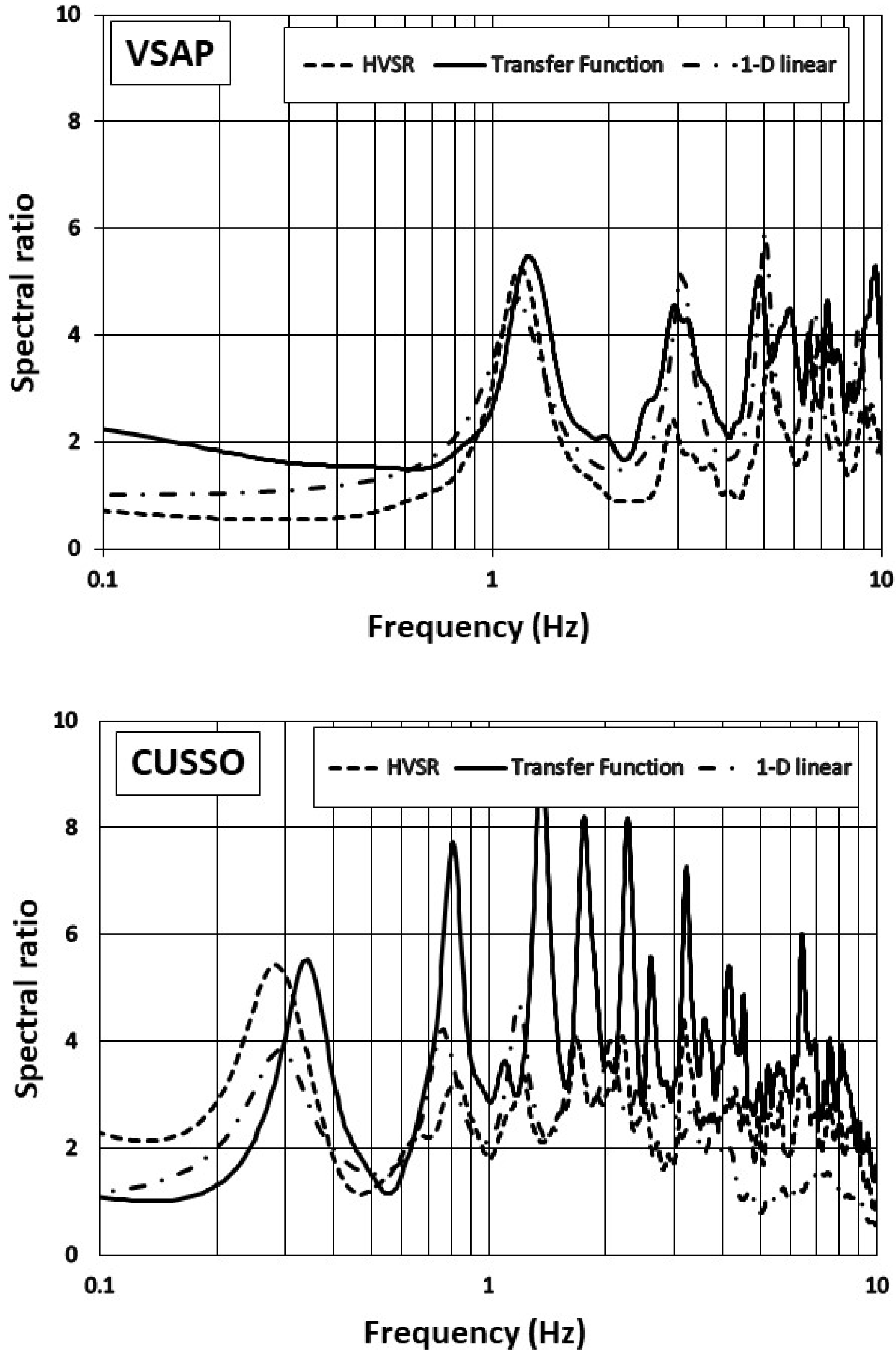


Figure 11. Comparisons between 1-D linear site responses, empirical transfer functions, and corrected HVSR curves for stations VSAP and CUSSO.

**Table 1.** National Earthquake Hazards Reduction Program site classification system for seismic design.

| *Site Class* | *Soil/Rock Description* | *$V_s30$ (m/s)* |
|---|---|---|
| A | Hard rock | >1,500 |
| B | Rock | 760–1,500 |
| C | Very dense soil/soft rock | 360–760 |
| D | Stiff soil | 180–360 |
| E | Soft soil | <180 |
| F | Special soils requiring site-specific analysis | |

**Table 2.** Short-period (0.2 s) site coefficient, $F_a$.

| *Site Class* | *Mapped Risk-Targeted Maximum Considered Earthquake Spectral Response Acceleration Parameter at Short Period (0.2 s)* | | | | |
|---|---|---|---|---|---|
| | $S_S \leq 0.25g$ | $S_S = 0.5g$ | $S_S = 0.75g$ | $S_S = 1.0g$ | $S_S \geq 1.25g$ |
| A | 0.8 | 0.8 | 0.8 | 0.8 | 0.8 |
| B | 1.0 | 1.0 | 1.0 | 1.0 | 1.0 |
| C | 1.2 | 1.2 | 1.1 | 1.0 | 1.0 |
| D | 2.4 | 1.6 | 1.4 | 1.2 | 1.0 |
| E | 2.5 | 1.7 | 1.2 | 0.9 | 0.9 |
| F | Special soils requiring site-specific analysis | | | | |
| Note: Use straight-line interpolation for intermediate values of $S_S$ | | | | | |

**Table 3.** 1.0 s period site coefficient, $F_V$.

| *Site Class* | *Mapped Risk-Targeted Maximum Considered Earthquake Spectral Response Acceleration Parameter at 1.0 s Period* | | | | |
|---|---|---|---|---|---|
| | $S_S \leq 0.25g$ | $S_S = 0.5g$ | $S_S = 0.75g$ | $S_S = 1.0g$ | $S_S \geq 1.25g$ |
| A | 0.8 | 0.8 | 0.8 | 0.8 | 0.8 |
| B | 1.0 | 1.0 | 1.0 | 1.0 | 1.0 |
| C | 1.7 | 1.6 | 1.5 | 1.4 | 1.3 |
| D | 2.4 | 2.0 | 1.8 | 1.6 | 1.5 |
| E | 3.5 | 3.2 | 2.8 | 2.4 | 2.4 |
| F | Special soils requiring site-specific analysis | | | | |
| Note: Use straight-line interpolation for intermediate values of $S_1$ | | | | | |

The $V_s30$ at stations VSAP and CUSSO (Fig. 4) are 291 m/s and 204 m/s, respectively, which classifies both as site class D according to Table 1. In other words, stations VSAP and CUSSO should have the same site response according to the NEHRP site classification. But, as shown in Figures 8–11, the site responses are different at the two stations, particularly the fundamental site frequencies: 1.1 Hz at station VSAP versus 0.3 Hz at station CUSSO. Thus, $V_s30$ may not be an appropriate parameter for capturing site response.

Figure 12a shows three shear-wave structures: one single layer, one two layers, and one gradient layer over a half space with shear-wave velocity of 800 m/s. All three velocity structures have the same $V_s30$ of 430 m/s. Figure 12b shows spectral amplifications for the three velocity structures using Thomson-Haskell propagator matrices. Even

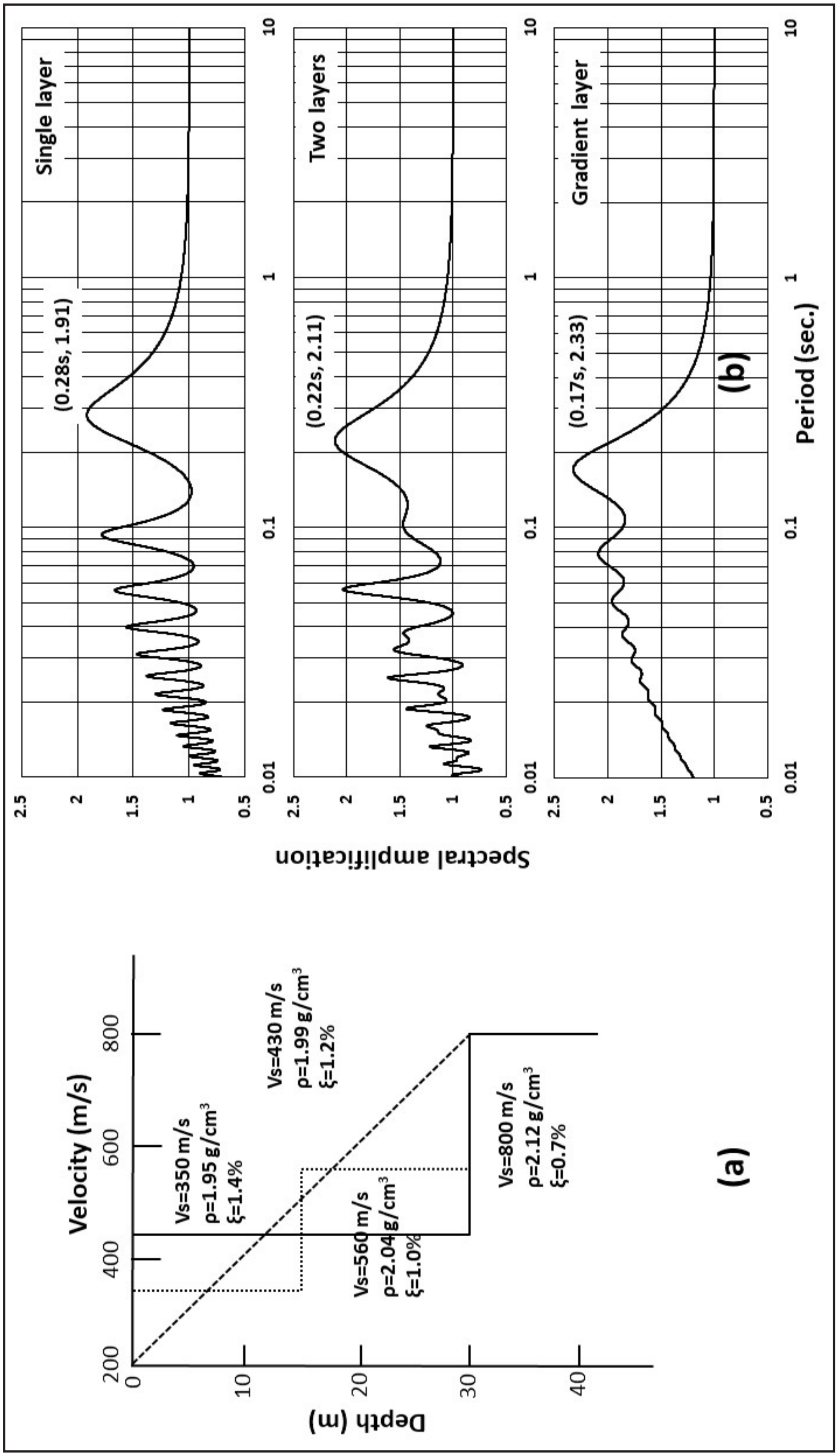


Figure 12. Three shear-wave velocity structures with the same $V_s30$ of 430 m/s (a) and their resulting 1-D linear spectral amplifications (b).

though the different velocity structures have the same $V_s30$ (Fig. 12a), they each generate a different site response: resonances with fundamental periods of 0.28 s and 0.22 s and peak amplifications of 1.91 and 2.11, respectively, for the structures with velocity contrasts, and amplification at shorter periods with a peak amplitude of 2.23 at a period of 0.17 s and no clear resonance for the gradient structure. Figure 12 demonstrates that the site responses (i.e., spectral amplifications) are uniquely determined by the velocity structures, but not $V_s30$. Thus, Figure 12 further demonstrates that $V_s30$ is not an appropriate parameter for capturing site response because there is no physical relationship between $V_s30$ and site response.

Therefore, the $V_s30$-based site correction factors (Tables 2–3) are not appropriate to use for accounting for site response in engineering design.

## Mapping Fundamental Site Period and Peak Amplification

As discussed earlier, site response is quantified by two parameters: the fundamental site frequency ($f_0$) or period ($T_f$) and peak amplification ($A_0$). Harris (1992) derived the thickness and average shear-wave velocity of the sediments for the Paducah metropolitan area from seismic-refraction/reflection profiles and produced a map of the linear (i.e., low-strain) fundamental site periods using equation 3 (Fig. 13). Street and others (1997a) derived site dynamic periods (Fig. 14) for the Jackson Purchase Region from measured shear-wave velocity profiles using 1-D equivalent-linear analysis—SHAKE91 (Idriss and Sun, 1992). No associated peak amplification was derived, however.

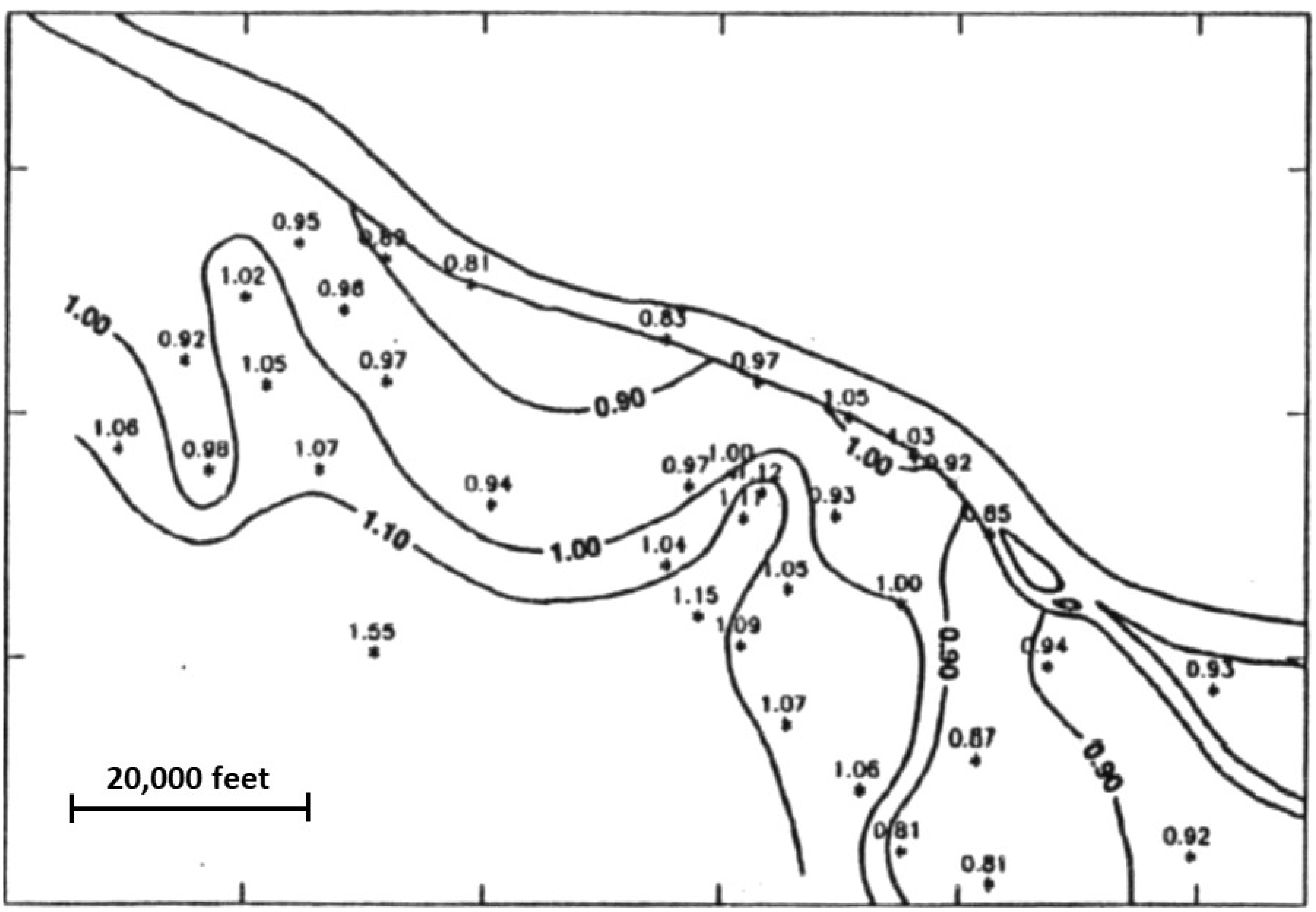


Figure 13. Linear fundamental site periods for the Paducah metropolitan area. Modified from Harris (1992). Used with permission.

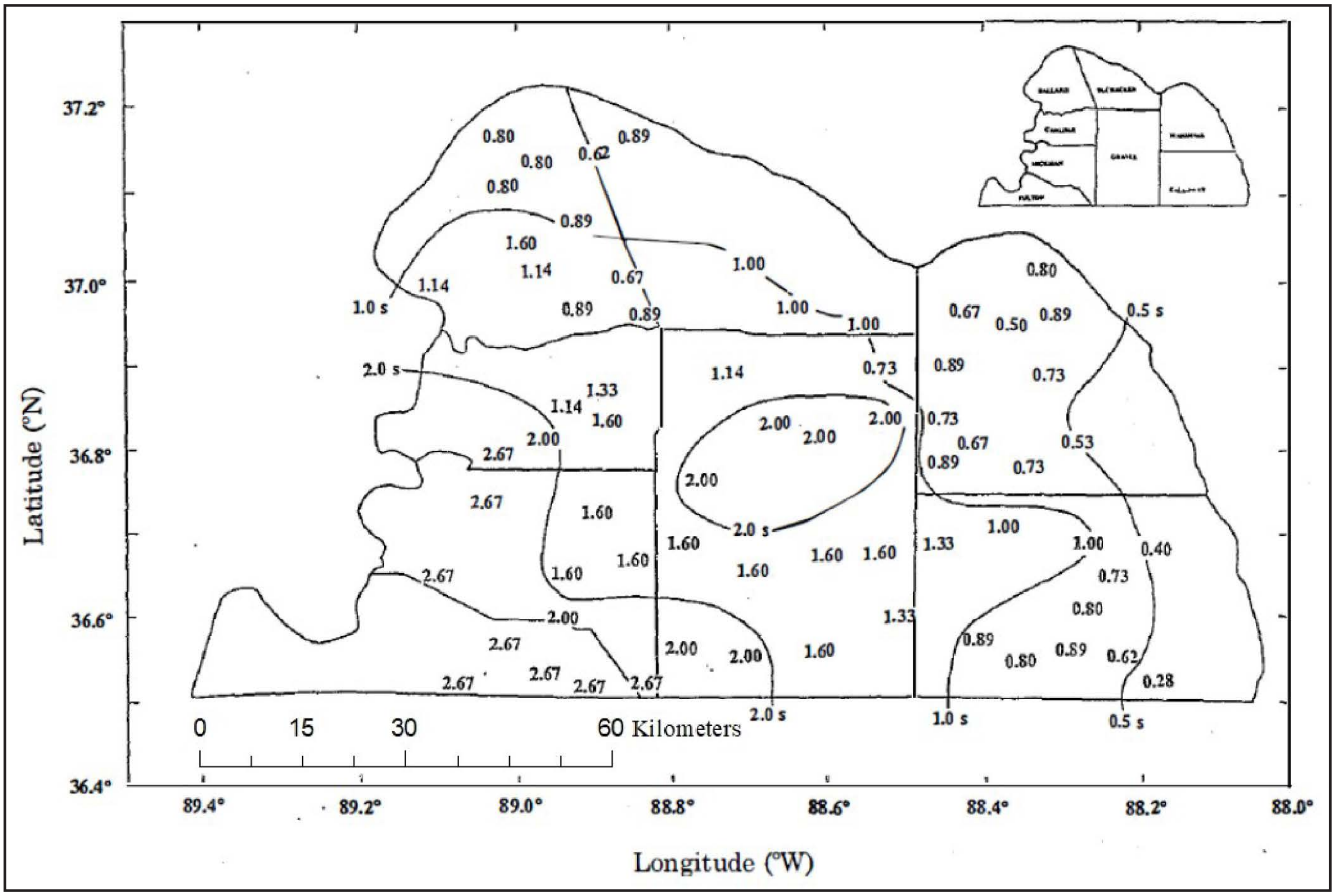


Figure 14. Linear fundamental site periods for the Jackson Purchase Region. Modified from Street and others (1997a). Used with permission.

We derived the linear fundamental site periods and peak amplifications for the Jackson Purchase Region using 1-D linear analysis—STRATA (Kottke and Rathje, 2009)—and the shear-wave velocity database accumulated at the University of Kentucky. The densities and damping ratios for the velocity profiles at each site were calculated from the shear-wave velocities based on the statistical relationships of Boore (2016) and Wang and others (1994). Figures 15 and 16 are contour maps of the fundamental site period and peak amplification for the Jackson Purchase Region derived from this study. Figure 15 shows that the fundamental site periods increase to the southwest or with an increase of sediment thickness (Fig. 2). The peak amplifications vary in the range of 4.0 to 8.0 in the region (Fig. 16).

## Summary

From January 2018 to December 2019, KGS monitored earthquakes and conducted research on seismic hazards, site response in particular, in the vicinity of the Paducah Gaseous Diffusion Plant. We gained a better understanding of ground-motion site response, particularly by the thick sediments, using data accumulated at the University of Kentucky. Our study has shown that the NEHRP site classification, which is based on $V_s30$, and correction factors are not appropriate to account for site response in engineering applications in the central United States. Our efforts have contributed to the development of a sound scientific basis for the seismic design parameters for buildings and facilities at the gaseous diffusion plant and for western Kentucky in general.

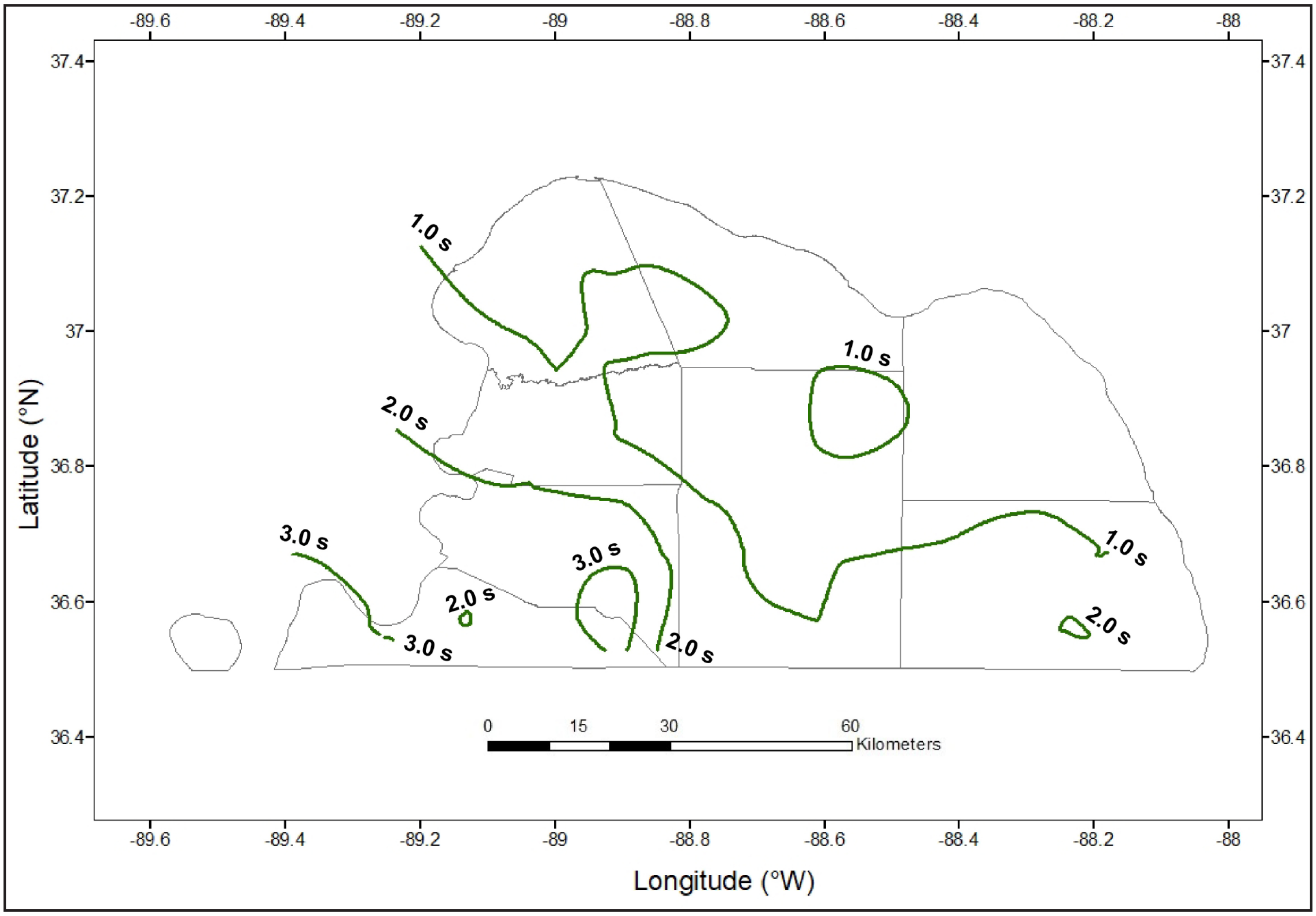


Figure 15. Linear fundamental site period trends for the Jackson Purchase Region derived from this study.


## Acknowledgments

John Hickman and Jason Dortch of KGS reviewed this report. We are grateful for their comments and suggestions, which helped improve this report.


## References Cited


American Society of Civil Engineers, 2010, Minimum design loads for buildings and other structures: American Society of Civil Engineers, ASCE/SEI 7-10, 209 p.

Asimaki, D., Mohammadi, K., Mason, B., Adams, R.K., and Khadka, D., 2017, Observations and simulations of basin effects in the Kathmandu Valley during the 2015 Gorkha earthquake sequence: Earthquake Spectra, v. 33, no. S1, p. S35–S53, https://doi.org/10.1193/013117eqs022m.

Boore, D.M., 2016, Determining generic velocity and density models for crustal amplification calculations, with an update of the Boore and Joyner (1997) generic site amplification for $(\overline{V}_S)(Z) = 760$ m/s: Bulletin of the Seismological Society of America, v. 106, p. 313–317, https://doi.org/10.1785/0120150229.

Boore, D.M., and Joyner, W.B., 1997, Site amplifications for generic rock sites: Bulletin of the Seismological Society of America, v. 87, p. 327–341.

Borcherdt, R.D., 1970, Effects of local geology on ground motion near San Francisco Bay: Bulletin of the Seismological Society of America, v. 60, p. 29–61.

Borcherdt, R.D., and Glassmoyer, G., 1992, On the characteristics of local geology and their influence on ground motions generated by the Loma Prieta earthquake in the San Francisco

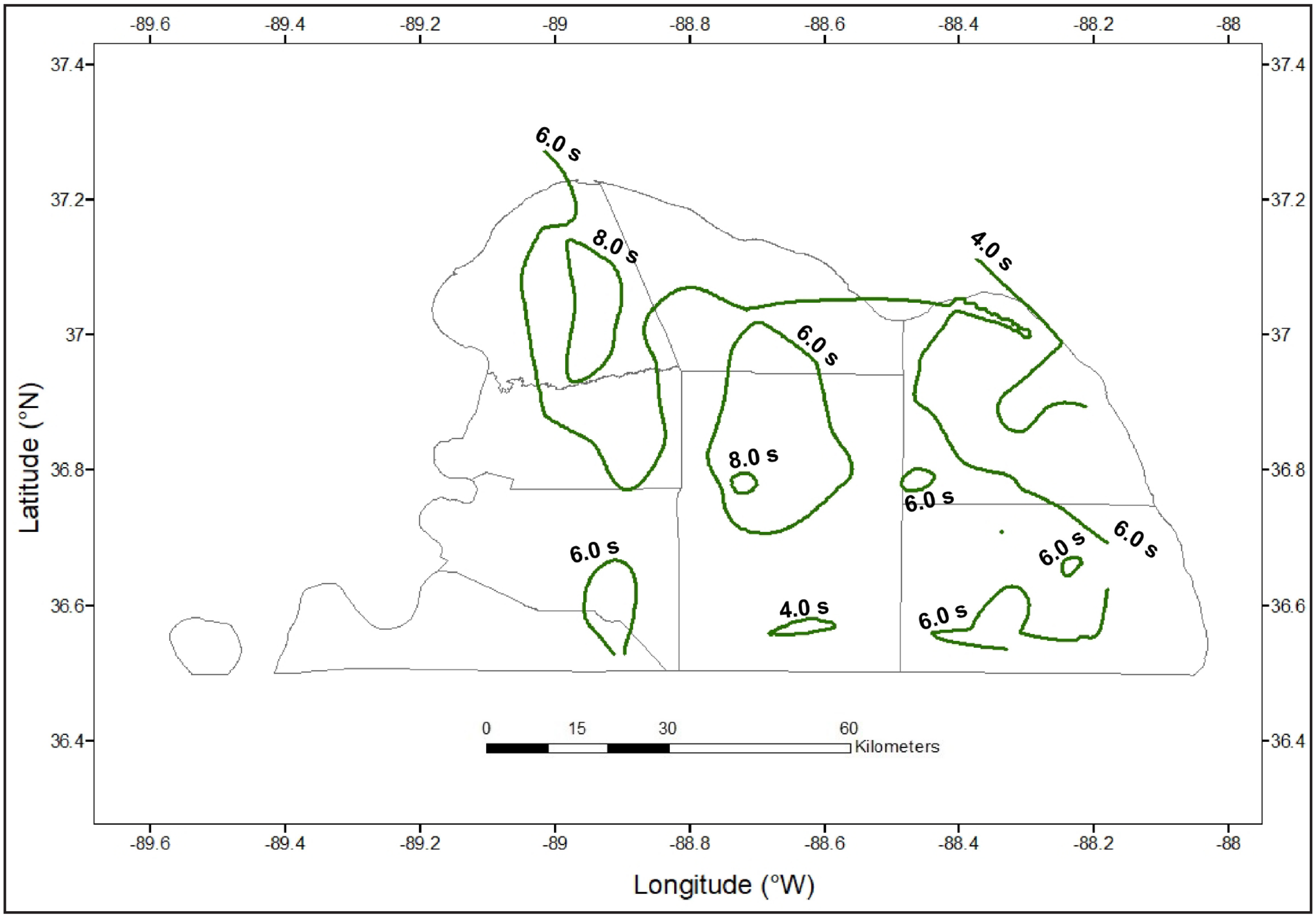


Figure 16. Peak amplifications trends for the Jackson Purchase Region derived from this study.


Bay region, California: Bulletin of the Seismological Society of America, v. 80, p. 603–641.

Building Seismic Safety Council, 1995, NEHRP recommended provisions for seismic regulations for new buildings [1994 ed.]: Federal Emergency Management Agency, FEMA 222, 290 p.

Building Seismic Safety Council, 2015, NEHRP recommended provisions for seismic regulations for new buildings [2015 ed.]: Federal Emergency Management Agency, FEMA P-1050, 555 p.

Carpenter, N.S., Wang, Z., and Woolery, E.W., 2020, An evaluation of linear site-response parameters in the central and eastern United States and the importance of empirical site-response estimations: Bulletin of the Seismological Society of America, v. 102, p. 1–19, doi:10.1785/0120190217.

Carpenter, N.S., Wang, Z., Woolery, E.W., and Rong, M., 2018, Estimating site response with recordings from deep boreholes and HVSR: Examples from the Mississippi Embayment of the central United States: Bulletin of the Seismological Society of America, v. 108, p. 1199–1209, doi:10.1785/0120170156.

Hardin, B.O., and Drnevich, V.P., 1972, Shear modulus and damping in soils: Design equations and curves: Journal of Soil Mechanics and Foundations Division, v. 98, p. 667–692.

Harris, J.B., 1992, Site amplification of seismic ground motions in the Paducah, Kentucky, area: Lexington, University of Kentucky doctoral dissertation, 367 p.

Harris, J., Street, R., Kiefer, J., Allen, D., and Wang, Z., 1994, Modeling site response in the Paducah, Kentucky, area: Earthquake Spectra, v. 10, p. 519–538.

Hartzell, S., Leeds, A., Frankel, A., and Michael, J., 1996, Site response for urban Los Angeles using aftershocks of the Northridge earthquake: Bulletin of the Seismological Society of America, v. 86, p. S168–S192.

Haskell, N.A., 1953, The dispersion of surface waves on multilayered media: Bulletin of the Seismological Society of America, v. 43, p. 17–34.

Haskell, N.A., 1960, Crustal reflection of plane SH waves: Journal of Geophysical Research, v. 65, p. 4147–4150.

Idriss, I.M., and Sun, J.I., 1992, User's manual for SHAKE91: University of California–Davis, Center for Geotechnical Modeling, Department of Civil and Environmental Engineering, 13 p.

International Code Council, 2011, 2012 international building code: International Code Council, 692 p.

Kottke, A.R., and Rathje, E.M., 2009, Technical manual for strata: University of California–Berkeley, Pacific Earthquake Engineering Research Center, PEER Report 2008/10, 103 p.

Lermo, J., and Chávez-García, F.J., 1993, Site effect evaluation using spectral ratios with only one station: Bulletin of the Seismological Society of America, v. 83, p. 1574–1594.

Lu, M., Li, X.J., An, X.W., and Zhao, J.X., 2010, A comparison of recorded response spectra from the 2008 Wenchuan, China, earthquake with modern ground-motion prediction models: Bulletin of the Seismological Society of America, v. 100, p. 2357–2380, https://doi.org/10.1785/0120090303.

Macpherson, K.A., Woolery, E.W., Wang, Z., and Liu, P., 2010, Three-dimensional long period ground motion simulations in the Upper Mississippi Embayment: Seismological Research Letters, v. 81, p. 391–405, doi:10.1785/gssrl.81.2.391.

Olive, W.W., 1972, Geology of the Jackson Purchase Region, Kentucky (roadlog for Geological Society of Kentucky 1972 field excursion): Kentucky Geological Survey, ser. 10, 11 p.

Olsen, K., 2000, Site amplification in the Los Angeles Basin from three-dimensional modeling of ground motion: Bulletin of the Seismological Society of America, v. 90, p. S77–S94, doi:10.1785/0120000506.

Ramirez-Guzman, L., Graves, R.W., Olsen, K.B., Boyd, O.S., Cramer, C., Hartzell, S., Ni, S., Somerville, P., Williams, R.A., and Zhong, J., 2015, Ground-motion simulations of 1811-1812 New Madrid earthquakes, central United States: Bulletin of the Seismological Society of America, v. 105, p. 1961–1988, doi:10.1785/0120140330.

Rodgers, A.J., Petersson, N.A., Pitarka, A., McCallen, D.B., Sjogreen, B., and Abrahamson, N., 2019, Broadband (0–5 Hz) fully deterministic 3D ground motion simulations of a magnitude 7.0 Hayward Fault earthquake: Comparison with empirical ground motion models and 3D path and site effects from source normalized intensities: Seismological Research Letters, v. 90, p. 1268–1284, doi:10.1785/0220180261.

Saikia, C.K., Pitarka, A., and Ichinose, G.A., 2006, Effects of irregular structure of the Mississippi Embayment on ground-motion amplification: Bulletin of the Seismological Society of America, v. 96, p. 1448–1473, doi:10.1785/0120050113.

Schnabel, P.B., Lysmer, J., and Seed, H.B., 1972, SHAKE: A computer program for earthquake response analysis of horizontally layered sites: University of California–Berkeley, Earthquake Engineering Research Center, Report No. UCB/EERC-72/12, 102 p.

Seed, H.B., Romo, M.P., Sun, J.I., Jaime, A., and Lysmer, J., 1988, The Mexico earthquake of September 19, 1985—Relationship between soil conditions and earthquake ground motions: Earthquake Spectra, v. 4, p. 687–729.

Street, R., Wang, Z., Woolery, E., Harik, I.E., Allen, D.L., and Sutterer, K.G., 1997a, Dynamic site periods for the Jackson Purchase Region of western Kentucky: Kentucky Transportation Center, Research Report KTC-97-1, 114 p.

Street, R., Wang, Z., Woolery, E., Hunt, J., and Harris, J., 1997b, Site effects at a vertical accelerometer array near Paducah, Kentucky: Engineering Geology, v. 46, p. 349–367.

Street, R., Woolery, E., Wang, Z., and Harik, I.E., 1997c, Soil classifications for estimating site-dependent response spectra and seismic coefficients for building code provisions in western Kentucky: Engineering Geology, v. 46, p. 331–347.

Street, R., Woolery, E., Wang, Z., and Harris, J., 2001, NEHRP soil classifications for estimating site-dependent seismic coefficients in the Upper Mississippi Embayment: Engineering Geology, v. 62, p. 123–135, https://doi.org/10.1016/S0013-7952(01)00057-6.

Wang, Z., comp., 2003, Proceedings of the Kentucky NEHRP Seismic Hazards and Design Maps Workshop, November 18, 2002, Lexington, Kentucky: Kentucky Geological Survey, ser. 12, Special Publication 5, 38 p.

Wang, Z., comp., 2005, Better understanding and communication of the national seismic hazard maps: Summary of USGS-KGS meeting on seismic hazard assessment in western Kentucky: Kentucky Geological Survey, ser. 12, Special Publication 7, 47 p.

Wang, Z., 2006, Understanding seismic hazard and risk assessments: An example in the New Madrid Seismic Zone of the central United States: Proceedings of the 8th U.S. National Conference on Earthquake Engineering, April 18–22, 2006, San Francisco, California, Paper 416, 10 p.

Wang, Z., 2007, Continental intraplate earthquakes: Science, hazard, and policy issues, *in* Stein, S., and Mazzotti, S., eds., Seismic hazard and risk assessment in the intraplate environment: The New Madrid Seismic Zone of the central United States: Geological Society of America Special Paper 425 p. 363–373, https://doi.org/10.1130/2007.2425(24).

Wang, Z., 2008, A technical note on seismic microzonation in the central United States: Journal of Earth System Science, v. 117, no. S2, p. 749–756, doi:10.1007/s12040-008-0060-8.

Wang, Z., 2010, Ground motion for the maximum credible earthquake in Kentucky: Kentucky Geological Survey, ser. 12, Report of Investigations 22, 9 p., https://doi.org/10.13023/kgs.ri22.12.

Wang, Z., 2011, Seismic hazard assessment: Issues and alternatives: Pure and Applied Geophysics, v. 168, p. 11–25, doi:10.1007/s00024-010-0148-3.

Wang, Z., Carpenter, N.S., and Woolery, E.W., 2019, An update of seismic monitoring and research in the vicinity of the Paducah Gaseous Diffusion Plant: January 2013–December 2017: Kentucky Geological Survey, ser. 13, Report of Investigations 6, 19 p., https://doi.org/10.13023/kgs.ri06.13.

Wang, Z., and Cobb, J.C., 2012, A critique of probabilistic versus deterministic seismic hazard analysis with special reference to the New Madrid Seismic Zone, *in* Cox, R.T., Tuttle, M.P., Boyd, O.S., and Locat, J., eds., Recent advances in North American paleoseismology and neotectonics east of the Rockies: Geological Society of America Special Paper 493, p. 259–275, doi:10.1130/2012.2493(13).

Wang, Z., and Lu, M., 2011, A short note on ground-motion recordings from the M7.9 Wenchuan, China, earthquake and ground-motion prediction equations in the central and eastern United States: Seismological Research Letters, v. 82, p. 731–733, doi:10.1785/gssrl.82.5.731.

Wang, Z., and Ormsbee, L., 2005, Comparison between probabilistic seismic hazard analysis and flood frequency analysis: Eos, Transactions of the American Geophysical Union, v. 86, p. 45, 51–52, https://doi.org/10.1029/2005EO050001.

Wang, Z., Street, R., Woolery, E., and Harris, J., 1994, $Q_s$ estimation for unconsolidated sediments using first arrival SH wave critical refractions: Journal of Geophysical Research: Solid Earth, v. 99, p. 13,543–13,551, https://doi.org/10.1029/94JB00499.

Wang, Z., and Woolery, E.W., 2006, Recordings from the deepest borehole in the New Madrid Seismic Zone: Seismological Research Letters, v. 77, p. 131–136, doi:10.1785/gssrl.77.2.148.

Wang, Z., and Woolery, E.W., 2008, Seismic hazard assessment of the Paducah Gaseous Diffusion Plant: Kentucky Geological Survey, ser. 12, Special Publication 9, 37 p.

Wang, Z., and Woolery, E., 2013, Operation and maintenance of the seismic network in the vicinity of the Paducah Gaseous Diffusion Plant: April 2009–September 2012: Kentucky Geological Survey, ser. 12, Contract Report 5, 11 p.

Wang, Z., Woolery, E.W., and Hu, C., 2012, The Central United States Seismic Observatory: Site characterization: Proceedings of the 5th International Conference on Environmental and Engineering Geophysics, June 15–18, 2012, Changsha, China, p. 223–227.

Wang, Z., Woolery, E.W., and Shi, B., 2003, Observed seismicity (earthquake activity) in the Jackson Purchase Region of western Kentucky: January through June 2003: Kentucky Geological Survey, ser. 12, Special Publication 6, 16 p.

Woolery, E.W., Lin, T., Wang, Z., and Shi, B., 2008, The role of local soil-induced amplification in the 27 July 1980 northeastern Kentucky earthquake: Environmental & Engineering Geoscience, v. 14, p. 267–280, doi:10.2113/gseegeosci.14.4.267.

Woolery, E.W., Wang, Z., and Carpenter, N.S., 2016a, Site characteristics, instrumentation, and recordings of the Central United States Seismic Observatory: Kentucky Geological Survey, ser. 12, Report of Investigations 37, 28 p., https://doi.org/10.13023/kgs.ri37.12.

Woolery, E.W., Wang, Z., Carpenter, N.S., Street, R., and Brengman, C., 2016b, The Central United States Seismic Observatory: Site characterization, instrumentation, and recordings: Seismological Research Letters, v. 87, p. 215–228, doi:10.1785/0220150169.

Zandieh, A., and Pezeshk, S., 2011, A study of horizontal-to-vertical component spectral ratio in the New Madrid Seismic Zone: Bulletin of the Seismological Society of America, v. 101, p. 287–296, doi:10.1785/0120100120.

Zhao, J.X., Irikura, K., Zhang, J., Fukushima, Y., Somerville, P.G., Asano, A., Ohno, Y., Oouchi, T., Takahashi, T., and Ogawa, H., 2006, An empirical site-classification method for strong-motion stations in Japan using H/V response spectral ratio: Bulletin of the Seismological Society of America, v. 96, p. 914–925.